

# Brain monoglyceride lipase participating in endocannabinoid inactivation

T. P. Dinh\*, D. Carpenter†, F. M. Leslie\*, T. F. Freund‡, I. Katona‡, S. L. Sensi\*<sup>§</sup>, S. Kathuria\*, and D. Piomelli\*<sup>¶</sup>

Departments of \*Pharmacology and †Neurology, University of California, Irvine, CA 92697-4625; ‡Institute of Experimental Medicine, Hungarian Academy of Sciences, Budapest 1450, Hungary; and §Department of Neurology, University G. d'Annunzio, Chieti 66013, Italy

Communicated by James L. McGaugh, University of California, Irvine, CA, June 4, 2002 (received for review February 22, 2002)

The endogenous cannabinoids (endocannabinoids) are lipid molecules that may mediate retrograde signaling at central synapses and other forms of short-range neuronal communication. The monoglyceride 2-arachidonoylglycerol (2-AG) meets several criteria of an endocannabinoid substance: (i) it activates cannabinoid receptors; (ii) it is produced by neurons in an activity-dependent manner; and (iii) it is rapidly eliminated. 2-AG inactivation is only partially understood, but it may occur by transport into cells and enzymatic hydrolysis. Here we tested the hypothesis that monoglyceride lipase (MGL), a serine hydrolase that converts monoglycerides to fatty acid and glycerol, participates in 2-AG inactivation. We cloned MGL by homology from a rat brain cDNA library. Its cDNA sequence encoded for a 303-aa protein with a calculated molecular weight of 33,367 daltons. Northern blot and *in situ* hybridization analyses revealed that MGL mRNA is heterogeneously expressed in the rat brain, with highest levels in regions where CB<sup>1</sup> cannabinoid receptors are also present (hippocampus, cortex, anterior thalamus, and cerebellum). Immunohistochemical studies in the hippocampus showed that MGL distribution has striking laminar specificity, suggesting a presynaptic localization of the enzyme. Adenovirus-mediated transfer of MGL cDNA into rat cortical neurons increased MGL expression and attenuated *N*-methyl-D-aspartate/carbachol-induced 2-AG accumulation in these cells. No such effect was observed on the accumulation of anandamide, another endocannabinoid lipid. The results suggest that hydrolysis by means of MGL is a primary mechanism for 2-AG inactivation in intact neurons.

Cannabinoid receptors, the molecular target for  $\Delta^9$ -tetrahydrocannabinol in marijuana, are activated by endogenous lipids that include the fatty ethanolamide, anandamide, and the monoglyceride, 2-arachidonoylglycerol (2-AG) (1–3). These compounds, collectively called endocannabinoids, are generated by cells on demand through stimulus-dependent cleavage of membrane phospholipid precursors and, after release, undergo rapid biological deactivation (4, 5). Because of their nonsynaptic production and fast elimination, the endocannabinoids are thought to act as short-range modulators of cell and synapse activity rather than classical hormones or neurotransmitters (for review, see ref. 6). In the brain striatum, for example, locally released anandamide may participate in an inhibitory feedback loop countering dopamine-induced facilitation of psychomotor activity (7, 8). Furthermore, in hippocampus and cerebellum, endogenously released 2-AG or anandamide produced from depolarized neurons may serve as a transsynaptic messenger, regulating neurotransmitter release (9–11) and influencing neuronal network activity (12, 13).

Anandamide and 2-AG are eliminated through a two-step process consisting of carrier-mediated transport into cells and subsequent enzymatic hydrolysis (for review, see ref. 14). In the brain, anandamide breakdown to arachidonic acid and ethanolamine is mediated by fatty acid amide hydrolase (FAAH), a member of the “amidase-signature family” of enzymes (15, 16). FAAH can function as a general hydrolytic enzyme not only for anandamide and other fatty ethanolamides but also for fatty esters such as 2-AG. This unusually broad substrate selectivity,

which was demonstrated in experiments with membrane and purified enzyme (17–19), has led researchers to suggest that FAAH may terminate the biological actions of both anandamide and 2-AG. Two findings, however, argue against this idea. First, a 2-AG hydrolase activity distinct from FAAH has been partially purified from porcine brain (20). Second, in intact astrocytoma cells, inhibition of FAAH activity prevents the hydrolysis of anandamide but not that of 2-AG (21). Thus, although 2-AG can be hydrolyzed by FAAH *in vitro*, different enzyme(s) may be responsible for its degradation *in vivo*. A possible candidate for this role is monoglyceride lipase (MGL), a serine hydrolase that cleaves 2- and 1-monoglycerides into fatty acid and glycerol (22). To test this hypothesis, we cloned rat brain MGL, determined its anatomical distribution, and used adenovirus-mediated gene transfer to investigate its role in neuronal 2-AG inactivation.

## Materials and Methods

**Cell Cultures.** We prepared and maintained primary cultures of cortical neurons from 18-day-old Wistar rat embryos as described (23); HeLa and COS-7 cells were purchased from American Type Culture Collection.

**cDNA Cloning and Adenovirus Preparation.** We used a 1-kb *Sma*I fragment from pBluescript-SK containing the full-length mouse adipocyte MGL cDNA (courtesy of C. Holm, Lund University, Lund, Sweden) to screen a rat brain cDNA library (Lambda Zap II, Stratagene) by low-stringency hybridization according to the manufacturer's instructions. On initial screening of  $2.5 \times 10^5$  phage plaques, we identified 40 positive clones, which we purified and subjected to secondary and tertiary screenings to ensure homogeneity. After phage purification, we excised insert-containing plasmids, transformed them into XL10-Gold ultra-competent bacteria (Stratagene), and conducted restriction analysis to identify positive clones. We selected for sequencing five random inserts that were greater than 1 kb in size. The inserts overlapped and together represented the entire ORF of MGL. To produce infectious adenovirus, we subcloned rat MGL cDNA into the plasmid pACYC (pACYC-MGL), cotransfected pACYC-MGL or pACYC (5  $\mu$ g each) with pJM17 into low-passage human embryonic kidney (HEK) 293 cells by calcium phosphate precipitation, and isolated adenovirus particles as described (24). The adenovirus stock was amplified and titered at the Viral Vector Center of the University of California, Irvine.

**Cell Infections and Incubations.** We infected HeLa cells for 2 h at 37°C with Ad5-Pac (control) or Ad5-MGL at a multiplicity of infection of 50 24 h before experiments and 4-day-old cortical neurons at a multiplicity of infection of 40 48 h before experiments. When appropriate, the neurons were labeled for 18–20 h with [<sup>3</sup>H]arachidonic acid (0.5  $\mu$ Ci; 100 Ci/mmol, American

Abbreviations: 2-AG, 2-arachidonoylglycerol; MGL, monoglyceride lipase; FAAH, fatty acid amide hydrolase; NMDA, *N*-methyl-D-aspartate.

Data deposition: The sequence reported in this paper has been deposited in the GenBank database (accession no. AY081195).

<sup>¶</sup>To whom reprint requests should be addressed. E-mail: piomelli@uci.edu.

Radiolabeled Chemicals, St. Louis, MO). To stimulate 2-AG formation maximally, we challenged the neurons with a combination of *N*-methyl-D-aspartate (NMDA) (300  $\mu$ M), carbachol (1 mM) and D-serine (100  $\mu$ M) (23).

**Antibody Generation.** A 15-aa peptide from the N-terminal region of MGL (SSPRTPQNVPYQDL) was synthesized and coupled to keyhole limpet hemocyanin by addition of a cysteine at the peptide N terminus (United Biochemical, Seattle). The conjugated peptide was injected into two rabbits to generate antisera (Strategic Biosolutions, Ramona, CA). We conjugated the peptide to an agarose column and purified the antiserum according to the manufacturer's instructions (AminoLink, Pierce Endogen, Rockford, IL).

**RNA and Protein Analyses.** We isolated total RNA (RNAqueous, Ambion, Austin, TX) from the brains of Wistar rats (250–300 g) and subjected it to Northern blot analyses (25) by using random-primed  $^{32}$ P-labeled cDNA probes for rat brain MGL or glycerol-aldehyde-3-phosphate dehydrogenase. We homogenized brains in Tris buffer (50 mM, pH 8.0) containing 0.32 M sucrose and prepared supernatant fraction by ultracentrifugation (100,000  $\times$  g). Protein concentration was determined with a Coomassie Plus kit (Pierce Endogen) by using BSA as standard. We electrophoresed supernatant proteins (50  $\mu$ g) on SDS-12% polyacrylamide gel, transferred them to Immobilon membranes (Millipore), and conducted Western blot analyses as described (26) by using an ECL-Plus kit (Amersham Pharmacia) to visualize immunoreactive bands.

**Lipid Analyses.** We extracted lipids with chloroform/methanol (2:1, vol/vol) and fractionated lipid products by TLC on silica gel G plates (EM Science) eluted with (i) ethyl acetate/methanol/water/ammonium hydroxide (20:1:10:1) or (ii) hexane/ethyl ether/acetic acid/methanol (85:20:2:4). When appropriate, we added as internal standards (1, 3) arachidonoylglycerol and arachidonic acid (20  $\mu$ g; Nu Check Prep, Elysian, MN). We visualized lipids with phosphomolybdic acid (10% in ethanol), scraped individual TLC bands, and measured radioactivity by liquid scintillation counting. HPLC/MS analyses were conducted as described (27).  $^2$ H<sub>4</sub>-labeled fatty ethanolamides were synthesized in the laboratory (28) and 2-[ $^2$ H<sub>8</sub>]AG was purchased from Cayman Chemical (Ann Arbor, MI).

**Enzyme Assays.** We incubated supernatant protein (50  $\mu$ g) in sodium phosphate buffer (50 mM, pH 8.0) with 2-oleoyl-[ $^3$ H]glycerol or 2-[ $^3$ H]AG (10  $\mu$ M; 5000 cpm, American Radiolabeled Chemicals) for 30 min at 37°C. This substrate concentration was selected to approximate 2-AG levels measured in brain slices after physiological stimulations (5). Assay duration, protein concentration, and buffer pH were selected on the basis of initial optimization tests (data not shown). The reactions were stopped, and products were separated by organic solvent extraction (chloroform/methanol, 1:1). When using 2-oleoyl-[ $^3$ H]glycerol, we measured released [ $^3$ H]glycerol in the aqueous phase by scintillation counting. When using 2-[ $^3$ H]arachidonoylglycerol, we subjected the organic phase to TLC fractionation and analyzed the products as described above. Hydrolysis of arachidonoyl-[ $^3$ H]ethanolamide ([ $^3$ H]anandamide) and palmitoyl-[ $^3$ H]ethanolamide (both from American Radiolabeled Chemicals) was measured in 50 mM Tris (pH 8.0) containing 10  $\mu$ M substrates (50,000 cpm) for 30 min at 37°C. Released [ $^3$ H]ethanolamine was measured in the aqueous phase after organic solvent extraction.

**Immunofluorescence Microscopy and *in Situ* Hybridization.** We cultured cortical neurons and HeLa cells on glass-bottom microwell dishes (MatTek Corporation, Ashland, MA), fixed them with 4%

paraformaldehyde in PBS at room temperature, permeabilized them with Triton X-100 (0.2%), and treated them with sodium borohydride (0.1%). After rinsing the cells with Tris-buffered saline, we incubated them for 60 min in PBS containing normal goat serum (10%) and BSA (1%) and incubated them overnight at 4°C with affinity-purified MGL antibody (1:2,500 dilution) in Tris-buffered saline containing BSA (1%). After rinsing with Tris-buffered saline, the cells were further incubated with goat anti-rabbit fluorescent-labeled secondary antibody (Alexa Fluor 488, Molecular Probes) and were immersed in mounting medium containing propidium iodide (1.5  $\mu$ g/ml) (Vectashield, Vector Laboratories, Burlingame, CA). Confocal experiments used an inverted laser scanning confocal microscope equipped with an argon laser (excitation 488 nm; emission >510 nm) and a 60 $\times$  epifluorescence oil immersion objective (Olympus, New Hyde Park, NY). Images were acquired and analyzed by using the dedicated OLYMPUS FLUOVIEW software. We conducted *in situ* hybridization experiments as described (29). We excised a  $\approx$ 500-bp *Bam*HI-*Xho*I MGL cDNA fragment from pBS-MGL and ligated it to *Bam*HI-*Xho*I-digested pBluescript-SK (pBS-MGL-IS). We prepared plasmid DNA by using a Qiagen Midi Plasmid Kit (Qiagen, Valencia, CA). Antisense and sense probes were synthesized from pBS-MGL-IS and labeled with [ $^{35}$ S]UTP (29).

**Immunohistochemistry.** We perfused five rats through the left ventricle with saline (1 min) followed by fixative (4% paraformaldehyde/0.1% glutaraldehyde/0.2% picric acid dissolved in 0.1 M PBS; 300 ml). The brains were dissected into blocks, sliced with a Vibratome into 60- $\mu$ m-thick coronal sections, and washed with PBS. The sections were incubated in ascending sucrose solutions in 0.1 M PBS (10% for 20 min; 30% for 3 h); freeze-thawed over liquid nitrogen; washed with 0.1 M PBS and 0.05 M Tris-buffered saline (pH 7.4); blocked in 4% BSA and incubated in anti-MGL antiserum (1:500; 48 h); incubated in biotinylated goat anti-rabbit IgG (1:400, 2 h; Vector Laboratories) and then with Elite ABC kit (1:500, 1.5 h; Vector). Diaminobenzidine was used as a chromagen for the immunoperoxidase reaction. Finally, the sections were treated with osmium tetroxide (1%, 40 min), dehydrated in ascending alcohol series, and embedded into Durcupan (ACM, Fluka, Buchs, Switzerland).

## Results

**Cloning of Rat Brain MGL.** The nucleotide and predicted amino acid sequence of rat brain MGL are shown in Fig. 1. On the basis of the deduced amino acid sequence, rat brain MGL comprises 303 amino acids with a molecular weight of 33,367 daltons. Alignment between rat brain and mouse adipocyte MGL revealed that the two sequences are 92% identical. The residues composing the catalytic triad are conserved, as are the GSXSG and HG dipeptide motifs commonly found in lipases (22). In keeping with this homology, rat MGL cDNA encoded for a functionally active enzyme, as demonstrated by transient expression in COS-7 cells (data not shown). Primary sequence analysis of rat MGL did not reveal any obvious posttranslational motif but disclosed several consensus sequences for phosphorylation by protein kinases, including Ca<sup>2+</sup>/calmodulin kinase II and protein kinases A and C.

Northern blots of total RNA from various brain regions showed a single transcript of  $\approx$ 4 kb, identical in size to that of mouse MGL (22) (Fig. 2*a*). Although MGL mRNA was present throughout the brain, expression levels differed among regions, being higher in cerebellum, cortex, and hippocampus; intermediate in thalamus and striatum; and lower in brainstem and hypothalamus (Fig. 2*a*). Densitometric measurements provided these average optical density values (in arbitrary units): cortex, 7.5; hippocampus, 6.8; cerebellum, 6.1; thalamus, 5.4; striatum,

```

ATGCGTGGAGCAAGTTCCACCGAGCGAACTCCACAGAACCTCCCTACCGAGACCTTCT 60
M P E A S S P R R T P Q N V P Y Q D L P 20
CACCTGGTCAATGCGGATGGACGTCCTCTTTGTAGTACTGGAGGCCCGCTGGCCAC 120
H L V N A D G Q Y L F C R Y W K P S G T 40
CCCAAGCCCTCATCTTCGTGTCCATGGAGCTGGGAAACACTGTGGCCGTTATGACGAG 180
P K A L I F V S [H G] A G E H C G R Y D E 60
CTGGCTCAGATGTTGAGAGGGCTGGACATCTGGTGTTCGCCATGACCATGTTGGCCAT 240
L A Q M L K R L L D K L V F A H R D H V S H 80
GGCAGAGCCGAGGAGGAGGATGGTGTATCGGACTTCCAGTITTTGTAGAGATTG 300
G Q S E G E R M V V S D F Q V F V R D L 100
TTGCAGCACGTGAACACGCTCCAGAGGACTACCCGAGGTCCCGCTTCTCCTCTGGG 360
L Q H V N T V Q K D Y P E V P V F L L G 120
CACTCCATGGGCGGTGCATCTCCATCTAGCAGCTGCAGAGAGACCAACCCACTTTCT 420
H S M G G A I S I L A A A E R P T H F S 140
GGCATGATCCTAATTTCACTCTGATCCTTCCCAATCCGGAATCTGCATCGACTTTGAG 480
G M I L I S P L I L A N P E S A S T L K 160
GTCCCTGCTGCAAACTGCTCAATTTTGTCTCCGCAACATATCTTGGGCGCATGAC 540
V L A A K L L N F V L P N I S L G R I D 180
TCCAGCGTCTGTCTCGAACAAGTGGAGGTTGACCTGTACAACCTCCGACCCACTCAT 600
S S V L S R N K S E V D L Y N S D P L I 200
TGCACGAGGCGGTGAGGATGCTTTGGCATCCAGCTGCTGAACTGTCTCGAGGGT 660
C H A G V K V C F G I Q L L N A V S R V 220
GAGCGAGCAATGCCAGGCTGACACTGCGGTCTCTGCTGCTGAGGTTCTGTGACCGG 720
E R A M P R L T L P F L L L Q G S A D R 240
CTTTCGACGAGGAGGCTGCTCACTGCTCATGGAATCATCCCGACTCAGGACAAACA 780
L C D S K G A Y L L M E S S P S Q D K T 260
CTCAAGATGATGAGGCTGCTCACTGCTCATGGAATCATCCCGACTCAGGACAAACA 840
L K M Y E G A Y H V L H K E L P E V T N 280
TCTGCTCCATGAAATAAGTGGTGTCTCACAGGATAGCAGTGGCAGGAGCTAGG 900
S V L H E I N T W V S H R I A V A G A R 300
TGCTACCTGGA 912
C L P * 302

```

**Fig. 1.** Nucleotide and deduced amino acid sequence of rat brain MGL cDNA. Closed circles mark amino acid residues comprising the putative catalytic triad. The HG dipeptide motif often found in lipases is boxed.

4.6; hypothalamus, 1.2; and brainstem, 1.0. Western blot analyses confirmed the presence of MGL protein in brain tissue. By using an immunopurified polyclonal antibody to the N-terminal sequence of rat MGL, we identified two protein bands migrating at  $\approx 35$  and  $\approx 37$  kDa on SDS-polyacrylamide gels (Fig. 2*b*). Both bands disappeared after adsorption with immunizing peptide (data not shown), indicating that they represented closely related MGL isoforms. These isoforms may arise from alternative splicing (30) or from as-yet-unidentified posttranslational modification(s).

**Brain Localization of MGL.** We found high levels of MGL mRNA throughout the rat brain cortex, with the signal mainly concentrated in layers IV, deep V, and VI (Fig. 3*a-c*); in the hippocampus, where it was especially conspicuous in the CA3 field (Fig. 3*c* and *e*); and in the cerebellum (Fig. 3*b*). MGL mRNA was also remarkably abundant in the anterior thalamus, particularly in the anterodorsal nucleus (Fig. 3*b*), whereas it was

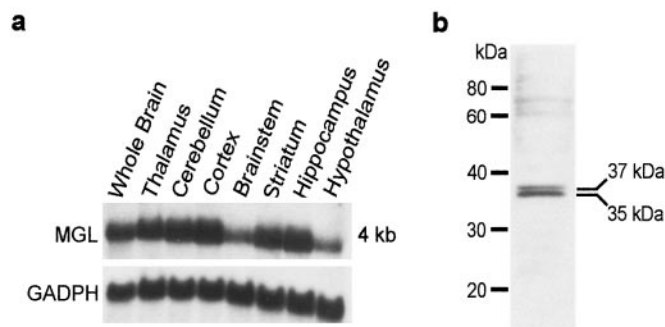


**Fig. 2.** MGL expression in the rat brain. (a) Northern blot analysis of MGL mRNA from various regions of the rat brain; glyceraldehyde-3-phosphate dehydrogenase mRNA was also measured to control for loading conditions. (b) Western blot analysis of soluble protein from rat brain, with an immunopurified polyclonal antibody to the N-terminal region of MGL. Both immunoreactive bands were abolished after adsorption with immunizing peptide (data not shown).

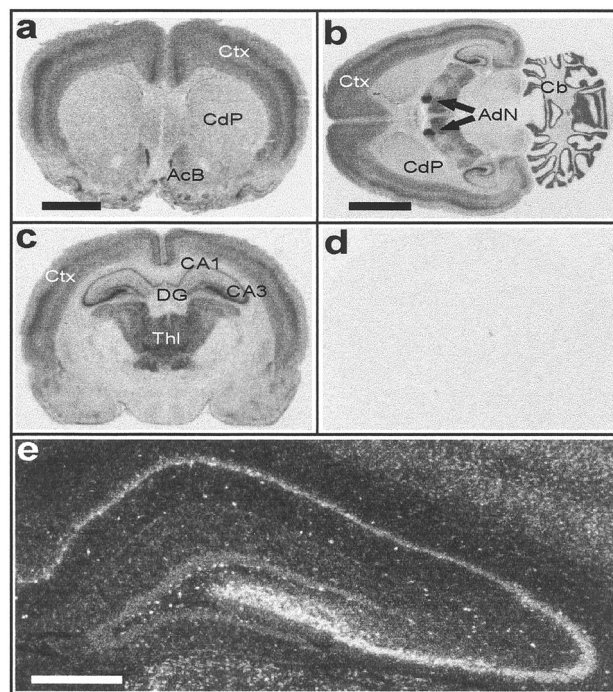


**Fig. 3.** Localization of MGL mRNA in the rat brain by *in situ* hybridization. Coronal (a and c) and horizontal (b) sections hybridized with an MGL antisense riboprobe labeled with [ $^{35}$ S]UTP. (d) Horizontal section hybridized with a sense probe. (e) Dark-field micrograph of MGL-positive cells in the hippocampus. ACB, nucleus accumbens; AdN, anterodorsal nucleus of the thalamus; Cb, cerebellum; CdP, caudate-putamen; Ctx, cortex; DG, dentate gyrus; Thl, thalamus. (Bar: a = 3 mm; b = 4 mm; e = 500  $\mu$ m.)

scarce in other thalamic areas (Fig. 3*b* and *c*). Moderate amounts of MGL mRNA were visible in the nucleus accumbens shell (Fig. 3*a*), islands of Calleja, and pontine nuclei (data not shown). No specific signal was visible in tissue sections hybridized with a sense probe (Fig. 3*d*).

Immunostaining of the hippocampus for MGL revealed a distinct laminar pattern, the most remarkable feature of which was a profound difference in staining intensity between the stratum radiatum, where the Schaffer collaterals terminate, and stratum lacunosum-moleculare, where the perforant pathway terminates (Fig. 4*a* and *b*). The neuropil of stratum oriens was also positive, whereas in stratum pyramidale, the MGL-negative pyramidal cell bodies were surrounded by positive basket cell terminals (Fig. 4*c*). In CA3, the strongly stained mossy fiber terminals in stratum lucidum, which are glutamatergic, were clearly discernible within the MGL-positive background (Fig. 4*c*). Mossy fiber collaterals and  $\gamma$ -aminobutyric acid-ergic basket cell axons were seen to surround somata and proximal dendrites also in the hilus of the dentate gyrus. Granule cell bodies were MGL-negative and surrounded by positive basket axons. In sections prepared by osmium treatment, the apical dendrites of pyramidal cells could be clearly followed in stratum radiatum, suggesting that the neuropil staining derived mostly, if not exclusively, from MGL localized in axon terminals (Fig. 4*d*). Antibody preadsorption with synthetic peptide resulted in complete loss of specific staining (data not shown).

**MGL Hydrolyzes 2-AG, Not Anandamide.** That FAAH hydrolyzes anandamide and 2-AG at comparable rates *in vitro* (17, 19) prompted us to examine whether brain MGL also recognizes anandamide. To this aim, we overexpressed MGL in HeLa cells by adenoviral vector-mediated gene transfer. In contrast with

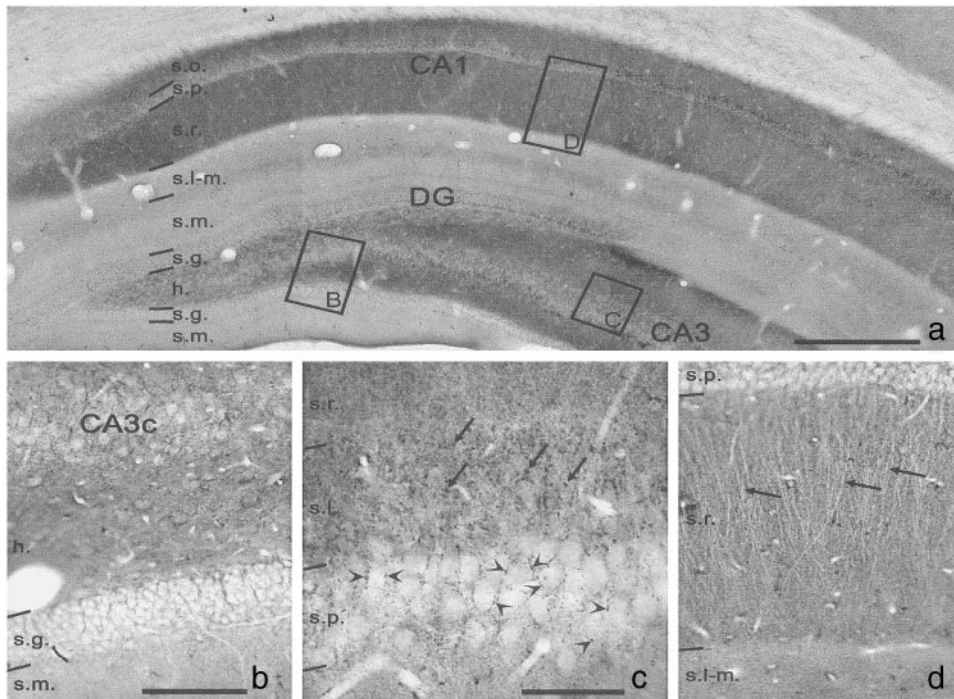


**Fig. 4.** Localization of MGL protein in the rat brain by immunohistochemistry. (a) Light micrograph of a hippocampal section immunostained for MGL revealing specific laminar distribution of the enzyme. At higher magnification (b–d), cell bodies of principal cells in all subfields are MGL-negative, but are surrounded by MGL-immunoreactive axon terminals (arrowheads in c) that resemble basket cell boutons. Mossy fiber terminals in CA3 stratum lucidum (arrows in c) are strongly immunostained. (d) Light micrograph of an osmium-treated section from CA1 shows that pyramidal dendrites in stratum radiatum (arrows) can be followed as negative images in the heavily stained neuropil. DG, dentate gyrus; h., hilus; s.g., stratum granulosum; s.l., stratum lucidum; s.l.m., stratum lacunosum-moleculare; s.m., stratum moleculare; s.o., stratum oriens; s.p., stratum pyramidale; s.r., stratum radiatum. (Bar: a, 500  $\mu\text{m}$ ; b–d, 100  $\mu\text{m}$ .)

vector-infected cells, cells infected with MGL-bearing adenovirus contained high levels of MGL immunoreactivity and enzyme activity (Fig. 5). MGL immunoreactivity was associated with both cell cytosol and plasma membranes (Fig. 5a); accordingly, after ultracentrifugation, MGL activity was recovered both in supernatant and particulate fractions (in picomol per minute per milligram of protein; supernatant: 0.28; particulate, 0.14;  $n = 3$ ). MGL activity was inhibited by various serine hydrolase inhibitors that were previously shown to block FAAH, including methyl arachidonylfluorophosphonate (half-maximal inhibitory concentration,  $\text{IC}_{50}$ ,  $0.8 \pm 0.05 \mu\text{M}$ ;  $n = 3$ ), arachidonyl trifluoromethylketone ( $\text{IC}_{50}$ ,  $2.5 \pm 0.04 \mu\text{M}$ ), and hexadecylsulfonyl fluoride ( $\text{IC}_{50}$ ,  $6.2 \pm 0.1 \mu\text{M}$ ). Nonradioactive 2-AG also inhibited the activity with an  $\text{IC}_{50}$  value of 3.3 mM. MGL hydrolyzed 2- $^3\text{H}$ ]AG and 2- $^3\text{H}$ ]OG, but not  $^3\text{H}$ ]anandamide or  $^3\text{H}$ ]palmitoylethanolamide (Fig. 3 and data not shown), indicating that the enzyme preferentially hydrolyzes 2-monoglycerides such as 2-AG over anandamide and other fatty ethanolamides.

**MGL Overexpression Curtails Receptor-Dependent 2-AG Accumulation.** Previous work has shown that coactivation of NMDA and cholinergic receptors stimulates the production and subsequent accumulation of 2-AG and anandamide in cortical neurons (23). If MGL selectively mediates 2-AG inactivation, changes in this enzyme activity should affect 2-AG accumulation but leaving anandamide's unchanged. To test this prediction, we induced MGL overexpression in neurons through adenoviral transfer. Compared with vector-infected neurons (Fig. 6a and b), neurons infected with MGL-bearing adenovirus contained substantially larger amounts of MGL mRNA (Fig. 6a) and protein (Fig. 6c). As expected, the main transcript in MGL-overexpressing neurons corresponded to the 1.2-kb coding sequence of MGL (Fig. 6a).

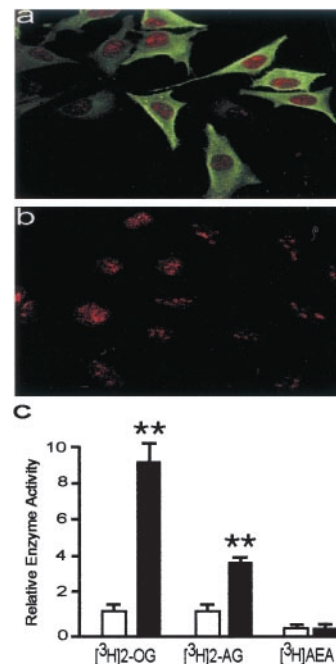


**Fig. 5.** Adenovirus-mediated MGL overexpression in HeLa cells. Confocal microscopy images of cells infected with MGL-containing (a) or control (b) adenovirus. MGL immunoreactivity is shown in green; cell nuclei in red. (c) MGL activity in vector (open bars)- or MGL (closed bar)-infected cells.  $^3\text{H}$ ]2-OG, 2-oleoyl- $^3\text{H}$ ]glycerol;  $^3\text{H}$ ]AEA,  $^3\text{H}$ ]anandamide. Results are expressed as the mean  $\pm$  SEM of three experiments performed in triplicate. \*\*,  $P < 0.01$ , Student's  $t$  test.

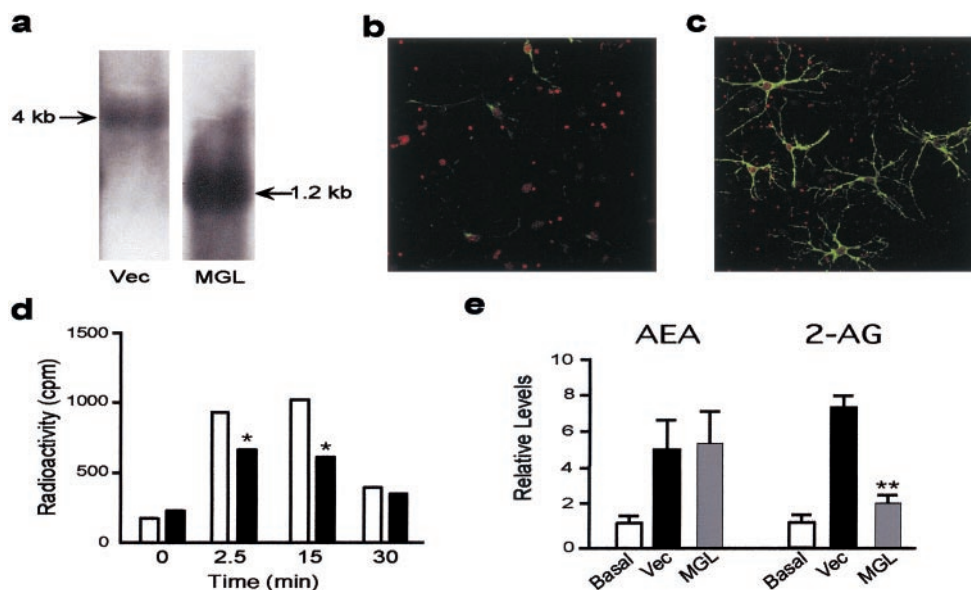


**Fig. 6.** Effects of MGL overexpression on receptor-dependent 2-AG accumulation in rat cortical neurons. Expression of MGL mRNA (a) and protein (b and c) in vector- and MGL-infected neurons. The 1.2-kb mRNA in overexpressing neurons corresponds to the coding sequence of MGL. Confocal microscopy images of vector- (b) and MGL (c)-infected neurons. Note the low, but detectable levels of endogenous MGL in vector-infected cells. MGL immunoreactivity is shown in green, cell nuclei in red. (d) Time course of 2-[<sup>3</sup>H]AG accumulation after coactivation of NMDA and cholinergic receptors in vector (open bars)- and MGL (filled bars)-infected neurons. Results are from one experiment, representative of four. (e) HPLC/MS quantitation of 2-AG and anandamide accumulation in neurons. Open bars, unstimulated vector-infected neurons; filled bars, stimulated vector-infected neurons; shaded bars, stimulated MGL-infected neurons. (Left) anandamide (AEA) levels; (Right) 2-AG levels. \*,  $P < 0.05$ ; \*\*,  $P < 0.01$ ;  $n = 5$ ; Student's  $t$  test.

In control neurons labeled by incubation with [<sup>3</sup>H]arachidonic acid, coactivation of NMDA and cholinergic receptors with NMDA/carbachol produces a rapid increase in 2-[<sup>3</sup>H]AG levels (Fig. 6d), which was significantly reduced in MGL-overexpressing neurons (Fig. 6d). This reduction likely reflects increased 2-AG breakdown rather than decreased 2-AG synthesis. Formation of 2-AG occurs by means of enzymatic hydrolysis of 1,2-diacylglycerol, which is generated through Ca<sup>2+</sup>-dependent cleavage of phosphoinositides by phospholipase C (5). These reactions were not affected by MGL overexpression; vector- and MGL-infected neurons had similar levels of stimulated 1,2-diacylglycerol production (vector: 6,700 ± 385 cpm per dish; MGL: 6,370 ± 440 cpm per dish;  $n = 8$ ) and [Ca<sup>2+</sup>]<sub>i</sub> rises (assessed by Fura-2 imaging; data not shown). Thus, MGL overexpression may promote 2-AG inactivation without affecting receptor-operated 2-AG formation. To determine whether this change is selective for 2-AG, we simultaneously measured 2-AG and anandamide by HPLC/MS. In vector-infected neurons, levels of both endocannabinoids increased markedly after a 2.5-min challenge with NMDA/carbachol (Fig. 6e). By contrast, in MGL-overexpressing cells, 2-AG accumulation was reduced 3-fold after the stimulation, although anandamide levels increased to the same extent as they did in vector-infected neurons (Fig. 6e). The results indicate that MGL catalyzes the hydrolysis of endogenously produced 2-AG, not anandamide, in intact neurons.

## Discussion

Understanding the molecular mechanisms that underlie endocannabinoid inactivation may have both experimental and clinical importance. Drugs targeting the biological disposition of anandamide and 2-AG may help unveil the physiological functions served by these lipid mediators and could offer a rational therapeutic approach to disease states, including pain (31) and stroke (32), in which endocannabinoids might play protective roles.

Significant insight has been gained recently into the process of anandamide inactivation, which is thought to require uptake into neurons and glia (33) mediated by a high-affinity transport system, followed by intracellular hydrolysis catalyzed by FAAH (15, 16, 34). The mechanisms responsible for 2-AG elimination, however, are still poorly understood. Although this monoglyceride may be taken up by brain cells through the same transport system as anandamide (21, 35), the identity of the intracellular enzyme(s) involved in 2-AG hydrolysis remains unresolved. 2-AG is a good substrate for FAAH in broken cell preparations (17, 18). However, brain tissue contains a 2-AG hydrolase activity that can be separated chromatographically from FAAH (20). Further, pharmacological inhibition of FAAH does not prevent 2-AG hydrolysis in intact astrocytoma cells (21). Even further, 2-AG hydrolysis is preserved in mutant mice lacking a functional FAAH (40). These findings suggest that an enzyme distinct from FAAH may be responsible for 2-AG hydrolysis *in vivo*. To test the hypothesis that MGL is such an enzyme, in the present study we have cloned rat brain MGL and examined its role in 2-AG deactivation.

By using adenovirus-mediated gene transfer, we found that MGL overexpression attenuates the NMDA/carbachol-induced accumulation of 2-AG in cortical neurons, but has no effect on either 2-AG synthesis or anandamide accumulation. We interpret these results to indicate that hydrolysis by MGL is a primary mechanism of 2-AG inactivation in intact neurons. Thus, 2-AG and anandamide may differ not only in their route of synthesis (4,5) but also in their intracellular inactivation.

In contrast to FAAH, which is widely distributed throughout the central nervous system (36), high levels of MGL mRNA are found in relatively few areas of the brain, including the hippocampus, cerebellum, anterodorsal nucleus of the thalamus, and cortex. That these brain regions also contain a high density of CB<sup>1</sup> receptors (37, 38) supports a role for MGL in terminating the cannabinergic effects of endogenously produced 2-AG. In the hippocampus, where such effects have been investigated in some detail, electrical stimulation of the

Schaffer collaterals, a glutamatergic fiber tract that projects from CA3 to CA1 field, enhances 2-AG synthesis (5). Newly generated 2-AG may in turn inhibit  $\gamma$ -aminobutyric acid release by CB<sup>1</sup> receptors on basket cell terminals (9, 10) and glutamate release by as-yet-unidentified CB<sup>1</sup>-like receptors on Schaffer terminals (39). Our results, showing that MGL is densely expressed in the termination zones of Schaffer collaterals, suggest a presynaptic localization of this enzyme and provide an anatomical locus for 2-AG deactivation at hippocampal synapses.

In conclusion, the *in situ* substrate specificity and discrete brain distribution of MGL, documented in the present study, underscore the role of this hydrolase in terminating 2-AG

signaling at cannabinoid receptors and highlight its significance as a target for pharmacological inhibition.

We thank Dr. Cecilia Holm (Lund University, Lund, Sweden) for the generous gift of mouse adipocyte MGL cDNA; Drs. M. L. Solbrig and A. Giuffrida for critical reading of the manuscript; Drs. F. Désarnaud, J. Fu, and C. Sanchez; and Y. Chen, S. Rao, D. Ton-That, and J. Yoo for experimental assistance. This work was supported by National Institute on Drug Abuse Grants 12447 and 3412 (to D.P.) and by the Howard Hughes Medical Institute and Orszgos Tudomnyos Kutatsi Alap (to T.F.F.). T.P.D. was supported by National Institute of Aging Fellowship AG00096, and S.L.S. was supported by National Institute of Aging Grant AG00919.

- Devane, W. A., Hanus, L., Breuer, A., Pertwee, R. G., Stevenson, L. A., Griffin, G., Gibson, D., Mandelbaum, A., Etinger, A. & Mechoulam, R. (1992) *Science* **258**, 1946–1949.
- Sugiura, T., Kondo, S., Sukagawa, A., Nakane, S., Shinoda, A., Itoh, K., Yamashita, A. & Waku, K. (1995) *Biochem. Biophys. Res. Commun.* **215**, 89–97.
- Mechoulam, R., Ben-Shabat, S., Hanus, L., Ligumsky, M., Kaminski, N. E., Schatz, A. R., Gopher, A., Almog, S., Martin, B. R., Compton, D. R., et al. (1995) *Biochem. Pharmacol.* **50**, 83–90.
- Di Marzo, V., Fontana, A., Cadas, H., Schinelli, S., Cimino, G., Schwartz, J. C. & Piomelli, D. (1994) *Nature (London)* **372**, 686–691.
- Stella, N., Schweitzer, P. & Piomelli, D. (1997) *Nature (London)* **388**, 773–778.
- Piomelli, D., Giuffrida, A., Calignano, A. & Rodríguez de Fonseca, F. (2000) *Trends Pharmacol. Sci.* **21**, 218–224.
- Giuffrida, A., Parsons, L. H., Kerr, T. M., Rodríguez de Fonseca, F., Navarro, M. & Piomelli, D. (1999) *Nat. Neurosci.* **2**, 358–363.
- Beltramo, M., Rodríguez de Fonseca, F., Navarro, M., Calignano, A., Gorriti, M. A., Grammatikopoulos, G., Sadile, A. G., Giuffrida, A. & Piomelli, D. (2000) *J. Neurosci.* **20**, 3401–3407.
- Wilson, R. I. & Nicoll, R. A. (2001) *Nature (London)* **410**, 588–592.
- Ohno-Shosaku, T., Maejima, T. & Kano, M. (2001) *Neuron* **29**, 729–738.
- Kreitzer, A. C. & Regehr, W. G. (2001) *Neuron* **29**, 717–727.
- Katona, I., Sperlagh, B., Sik, A., Kafalvi, A., Vizi, E. S., Mackie, K. & Freund, T. F. (1999) *J. Neurosci.* **19**, 4544–4558.
- Hajos, N., Katona, I., Naiem, S. S., MacKie, K., Ledent, C., Mody, I. & Freund, T. F. (2000) *Eur. J. Neurosci.* **12**, 3239–3249.
- Giuffrida, A., Beltramo, M. & Piomelli, D. (2001) *J. Pharm. Exp. Ther.* **298**, 7–14.
- Cravatt, B. F., Giang, D. K., Mayfield, S. P., Boger, D. L., Lerner, R. A. & Gilula, N. B. (1996) *Nature (London)* **384**, 83–87.
- Cravatt, B. F., Demarest, K., Patricelli, M. P., Bracey, M. H., Giang, D. K., Martin, B. R. & Lichtman, A. H. (2001) *Proc. Natl. Acad. Sci. USA* **98**, 9371–9376.
- Goparaju, S. K., Ueda, N., Yamaguchi, H. & Yamamoto, S. (1998) *FEBS Lett.* **422**, 69–73.
- Lang, W., Qin, C., Lin, S., Khanolkar, A. D., Goutopoulos, A., Fan, P., Abouzid, K., Meng, Z., Biegel, D. & Makriyannis, A. (1999) *J. Med. Chem.* **42**, 896–902.
- Patricelli, M. P. & Cravatt, B. F. (1999) *Biochemistry* **38**, 14125–14130.
- Goparaju, S. K., Ueda, N., Taniguchi, K. & Yamamoto, S. (1999) *Biochem. Pharmacol.* **57**, 417–423.
- Beltramo, M. & Piomelli, D. (2000) *NeuroReport* **11**, 1231–1235.
- Karlsson, M., Contreras, J. A., Hellman, U., Tornqvist, H. & Holm, C. (1997) *J. Biol. Chem.* **272**, 27218–27223.
- Stella, N. & Piomelli, D. (2001) *Eur. J. Pharmacol.* **425**, 189–196.
- Zuo, Z., Wang, C., Carpenter, D., Okada, Y., Nicolaidou, E., Toyoda, M., Trento, A. & Jordan, S. C. (2001) *Transplantation* **71**, 686–691.
- Maniatis, T., Sambrook, J. & Fritsch, E. F. (1989) *Molecular Cloning: A Laboratory Manual* (Cold Spring Harbor Lab. Press, Plainview, NY), 2nd Ed., Vol. 1, pp. 7.43–7.45.
- Maniatis, T., Sambrook, J. & Fritsch, E. F. (1989) *Molecular Cloning: A Laboratory Manual* (Cold Spring Harbor Lab. Press, Plainview, NY), 2nd Ed., Vol. 3, pp. 18.47–18.75.
- Giuffrida, A., Rodríguez de Fonseca, F. & Piomelli, D. (2000) *Anal. Biochem.* **280**, 87–93.
- Giuffrida, A., Rodríguez de Fonseca, F., Nava, F., Loubet-Lescoulié, P. & Piomelli, D. (2000) *Eur. J. Pharmacol.* **408**, 161–168.
- Winzer-Serhan, U. H., Broide, R. S., Chen, Y. & Leslie, F. M. (1999) *Brain Res. Protoc.* **3**, 229–241.
- Karlsson, M., Reue, K., Xia, Y. R., Lusia, A. J., Langin, D., Tornqvist, H. & Holm, C. (2001) *Gene* **272**, 11–18.
- Iversen, L. & Chapman, V. (2002) *Curr. Opin. Pharmacol.* **2**, 50–55.
- Panikashvili, D., Simeonidou, C., Ben-Shabat, S., Hanus, L., Breuer, A., Mechoulam, R. & Shohami, E. (2001) *Nature (London)* **413**, 527–531.
- Beltramo, M., Stella, N., Calignano, A., Lin, S. Y., Makriyannis, A. & Piomelli, D. (1997) *Science* **277**, 1094–1097.
- Ueda, N., Yamanaka, K. & Yamamoto, S. (2001) *J. Biol. Chem.* **276**, 35552–35557.
- Piomelli, D., Beltramo, M., Glasnapp, S., Lin, S. Y., Goutopoulos, A., Xie, X. Q. & Makriyannis, A. (1999) *Proc. Natl. Acad. Sci. USA* **96**, 5802–5807.
- Thomas, E. A., Cravatt, B. F., Danielson, P. E., Gilula, N. B. & Sutcliffe, J. G. (1997) *J. Neurosci. Res.* **50**, 1047–1052.
- Herkenham, M., Lynn, A. B., Johnson, M. R., Melvin, L. S., de Costa, B. R. & Rice, K. C. (1991) *J. Neurosci.* **11**, 563–583.
- Tsou, K., Brown, S., Sañudo-Peña, M. C., Mackie, K. & Walker, J. M. (1998) *Neuroscience* **83**, 393–411.
- Hajos, N., Ledent, C. & Freund, T. F. (2001) *Neuroscience* **106**, 1–4.
- Lichtman, A. H., Hawkins, E. G., Griffin, G. & Cravatt, B. F. (2002) *J. Pharmacol. Exp. Ther.* **302**, 73–79.